

# Journal of Photonics for Energy

SPIEDigitalLibrary.org/jpe

## **Electronic structure of molybdenum-oxide films and associated charge injection mechanisms in organic devices**

Jens Meyer  
Antoine Kahn



# Electronic structure of molybdenum-oxide films and associated charge injection mechanisms in organic devices

Jens Meyer and Antoine Kahn

Princeton University, Department of Electrical Engineering, Princeton, New Jersey, 08544  
[kahn@princeton.edu](mailto:kahn@princeton.edu)

**Abstract.** We report on the electronic structure of freshly evaporated and air-exposed Molybdenum tri-oxide ( $\text{MoO}_3$ ) and the energy-level alignment between this compound and a hole-transport material [e.g., *N,N'*-diphenyl-*N,N'*-bis (1-naphthyl)-1,1'-biphenyl-4,4'-diamine ( $\alpha$ -NPD)]. Ultraviolet and inverse photoelectron spectroscopy show that freshly evaporated  $\text{MoO}_3$  exhibits deep-lying electronic states with an electron affinity (EA) of 6.7 eV and ionization energy (IE) of 9.7 eV. Air exposure reduces EA and IE by  $\sim 1$  eV, to 5.5 and 8.6 eV, respectively, but does not affect the hole-injection efficiency, which is confirmed by device studies. Thus,  $\text{MoO}_3$  can be applied in low-vacuum environment, which is particularly important for low-cost manufacturing processes. Our findings of the energy-level alignment between  $\text{MoO}_3$  and  $\alpha$ -NPD also leads to a revised interpretation of the charge-injection mechanism, whereby the hole-injection corresponds to an electron extraction from the organic highest-occupied molecular orbital (HOMO) level via the  $\text{MoO}_3$  conduction band. © 2011 Society of Photo-Optical Instrumentation Engineers (SPIE). [DOI: [10.1117/1.3555081](https://doi.org/10.1117/1.3555081)]

**Keywords:** molybdenum oxide;  $\text{MoO}_3$ ; energy levels; ultraviolet photoelectron spectroscopy; inverse photoelectron spectroscopy; organic electronics.

Paper 10164SSPR received Sep. 15, 2010; revised manuscript received Jan. 26, 2011; accepted for publication Jan. 26, 2011; published online Mar. 10, 2011.

## 1 Introduction

Transition metal oxides (TMO) such as molybdenum oxide ( $\text{MoO}_3$ ), vanadium oxide ( $\text{V}_2\text{O}_5$ ), or tungsten oxide ( $\text{WO}_3$ ), have been extensively researched over the past few years as possible high-work-function (WF) hole-injection (extraction) materials for organic electronics. It is thought that the use of TMOs can lead to a significant performance enhancement of organic light-emitting diodes (OLED), organic transistors and organic photovoltaic cells (OPV).<sup>1-4</sup> TMOs, such as  $\text{MoO}_3$ , are also interesting from a device engineering standpoint in view of their high transparency in the visible region of the spectrum, nontoxicity and moderate evaporation temperatures compared to other metal oxides.

In early reports, the enhanced device efficiency due a  $\text{MoO}_3$  interlayer was attributed to the large work function ( $>5.0$  eV) exhibited by thin films of this material and to an electronic structure believed to correspond to an electron affinity (EA) and ionization energy (IE) of the order of 2.3 eV and 5.3–5.4 eV, respectively.<sup>1,5-7</sup> Accordingly,  $\text{MoO}_3$  was assumed to be a large gap, *p*-doped material, with the Fermi level close to the valence-band maximum.  $\text{MoO}_3$ -mediated hole injection would proceed by hole transfer through the oxide valence-band maximum, and the large gap and high conduction-band minimum would insure electron blocking in typical OPV structures. However, recent detailed investigations of  $\text{MoO}_3$  and  $\text{WO}_3$  vacuum-evaporated films<sup>8-11</sup> have provided strong evidence for a very different picture [i.e., strongly *n*-doped materials (via oxygen vacancies)], leading to considerably larger values of IE and EA.

These drastically different values have forced a complete reevaluation of the role of these TMO layers in organic devices.

In this paper, we review recent spectroscopy work via ultraviolet and inverse photoemission spectroscopy (UPS, IPES) measurements, that demonstrate that freshly evaporated (clean) MoO<sub>3</sub> exhibits EA, WF, and IE values of 6.7, 6.9, and 9.7 eV, respectively. We then further demonstrate that these values are reduced by air exposure, but that the material remains strongly *n*-type. The injection properties of clean and contaminated MoO<sub>3</sub> layers were studied in hole-only devices, demonstrating that even air-exposed films can act as a very efficient injection layer. On the basis of our finding, we revise the mechanism of MoO<sub>3</sub> hole-injection layers and present a model that is valid for clean and contaminated MoO<sub>3</sub> films as well.

## 2 Experimental

All the MoO<sub>3</sub> films used in this study were grown by vacuum evaporation from a source of MoO<sub>3</sub> powder (99.99% Sigma-Aldrich) in a growth chamber with base pressure of the order of 10<sup>-9</sup> Torr. The films were then directly transferred to an analysis chamber without ambient exposure or exposed for several minutes to ambient atmosphere to test for the impact of surface contamination on the electronic properties. Organic films were deposited either by vacuum evaporation for small molecules [e.g., *N,N'*-diphenyl-*N,N'*-bis(1-naphthyl)-1,1'-biphenyl-4,4'-diamine ( $\alpha$ -NPD)] or spin-coating for polymer films [e.g., poly(9,9'-dioctylfluorene-co-bis-*N,N'*-(4-butylphenyl)diphenylamine) (TFB)]. Current–voltage measurements were done using top vacuum-deposited Au pads or a mercury probe. UPS measurements were done using the He I (21.22 eV) and He II (40.8 eV) photon lines from a discharge lamp. The IPES experiments were done in the isochromat mode, using a setup described elsewhere.<sup>12</sup> The experimental resolution in UPS and IPES were 0.15 and 0.45 eV, respectively.

## 3 Results

The UPS and IPES spectra of freshly evaporated MoO<sub>3</sub> are shown in Fig. 1. The left panel displays the photoemission cutoff, whereas the right panel depicts the spectra of the density of states near the oxide valence-band (VB) and conduction-band (CB) edge. The photoemission cutoff is found at a value of 14.3 eV, which corresponds to a WF of 6.9 eV. The VB maximum is 2.8 eV below the Fermi level ( $E_F$ ) and corresponds to an IE of 9.7 eV. Via IPES measurements,

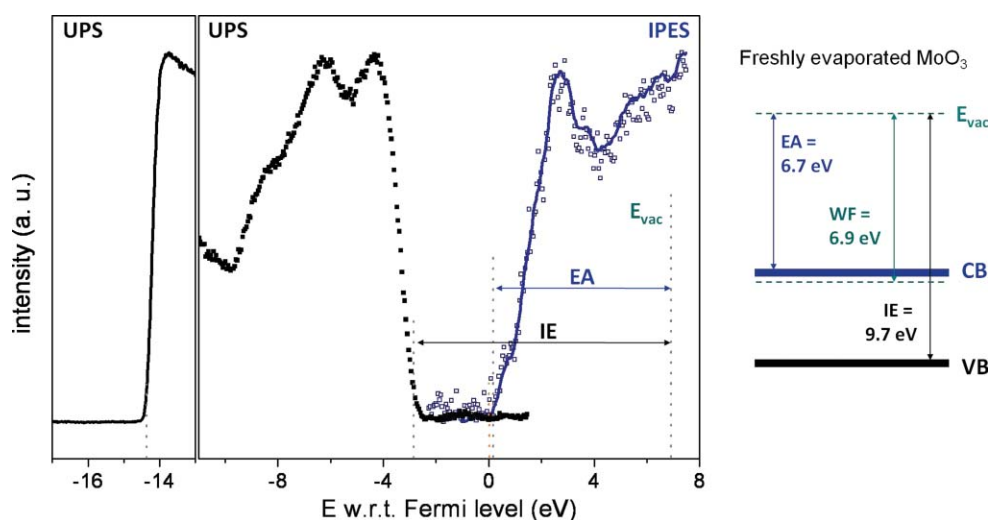


**Fig. 1** (Left) UPS and IPES spectra of clean MoO<sub>3</sub>. (Right) Schematic energy diagram, showing the IE, WF, and EA of the MoO<sub>3</sub> film.

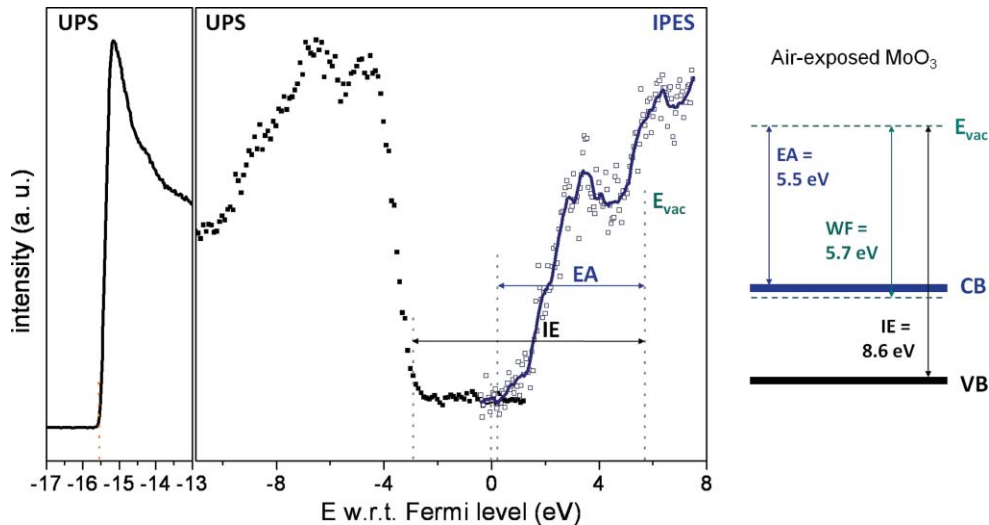


**Fig. 2** (Left) UPS and IPES spectra of clean MoO<sub>3</sub>. (Right) Scheme of corresponding energy level.

we find that the CB minimum is placed at  $\sim 0.2$  eV above  $E_F$ , resulting in an EA of 6.7 eV. The energy levels are summarized in the schematic of Fig. 1. The two most important and obvious features are that MoO<sub>3</sub> exhibits a large WF and very deep-lying electronic states, and is strongly *n*-type, presumably due to oxygen vacancies. Because a corollary of the fact that the EA is very large (i.e. 6.7 eV), electron-transport states (e.g., lowest unoccupied molecular orbitals) of other materials in contact with MoO<sub>3</sub> are unlikely to overlap with the 3 eV bandgap of MoO<sub>3</sub>, and the TMO cannot serve as an electron-blocking agent in organic (photovoltaic) devices, as had been frequently assumed in the literature. Furthermore, the charge transport presumably proceeds via the MoO<sub>3</sub> CB, rather than through its VB.

Before we address this latter issue in more detail, we look at the impact of contamination of the WF and energy levels of the film. The UPS and IPES spectra of a MoO<sub>3</sub> surface exposed for a relatively short period (3 min) to ambient air are shown in Fig. 2. Compared to the case of the freshly evaporated, unexposed, MoO<sub>3</sub> surface, the photoemission cutoff shifts toward lower binding energies, indicating a reduced WF of 5.7 eV. Corresponding to this vacuum-level shift of  $\sim 1$  eV, reduced values of 8.6 and 5.5 eV are obtained for IE and EA, respectively. However, the values WF and EA remain very close, indicating that the air-exposed contaminated MoO<sub>3</sub> film is highly *n*-type doped. The decrease of WF, IE, and EA on air exposure is attributed to adsorption of various species, such as water on the surface, and a corresponding lowering of the vacuum level. Incidentally, the fact that a short exposure to air already leads to a significant shift of the vacuum level, explains the large spread of reported WF values in the literature. These discrepancies originate with the varying environmental conditions in surface preparations and measurement techniques.

We previously reported on the interface energy-level alignment between the hole transport material  $\alpha$ -NPD and freshly evaporated versus air exposed MoO<sub>3</sub>.<sup>8,9</sup> Note that the WF of MoO<sub>3</sub> is larger than the IE of  $\alpha$ -NPD ( $\sim 5.5$  eV), whether the TMO film is exposed to ambient or not. As a consequence, the MoO<sub>3</sub>/ $\alpha$ -NPD interface barrier (i.e., the energy difference between the organic molecular levels and the TMO Fermi level) and CB is found to be independent of whether the metal oxide is contaminated or not. Only the interface dipole changes, as it compensates for the difference between these energy levels. This finding is confirmed by current-voltage ( $J$ - $V$ ) studies on simple devices [Fig. 3(a)]. The  $J$ - $V$  characteristics are obtained for hole-only devices (structure illustrates in inset), when a positive voltage is applied to the Au bottom electrode. It can clearly be seen that both clean and contaminated MoO<sub>3</sub> layers allow for a nearly identical

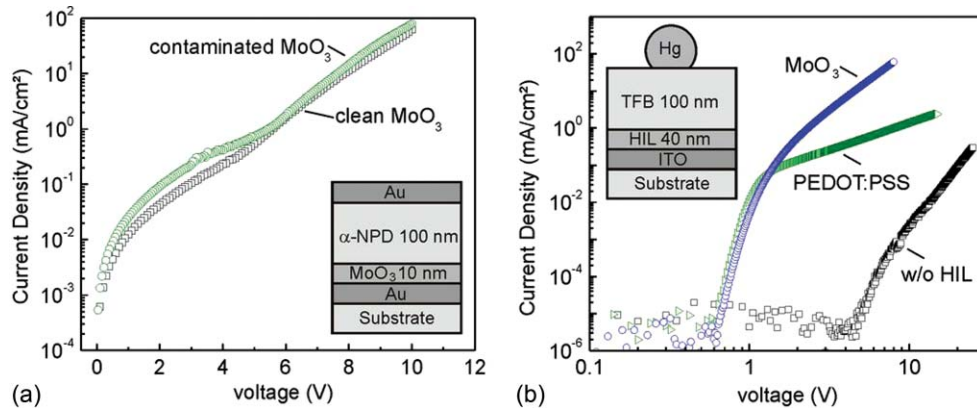


**Fig. 3** (a)  $J-V$  characteristics of hole-only devices comprising clean or air-exposed  $\text{MoO}_3$  and a vacuum-deposited  $\alpha$ -NPD layer (after Ref. 9); (b)  $J-V$  characteristics for hole injection into TFB without and with a HIL. The HIL is either PEDOT:PSS or  $\text{MoO}_3$  (after Ref. 13).

and also highly efficient hole-injection into  $\alpha$ -NPD. In addition, the study demonstrates that contaminated  $\text{MoO}_3$  can be used as efficient hole-injection material for a low-cost manufacturing process in low- or nonvacuum environment.

The results reported above lead to a revision of the charge injection mechanism, when  $\text{MoO}_3$ , or films of other TMOs like  $\text{WO}_3$ , are used to enhance hole injection. All the spectroscopy measurements on interfaces between hole transport materials and  $\text{MoO}_3$  (or  $\text{WO}_3$ ) interfaces point to the fact that the energy barrier between the CB of the TMO and the highest occupied molecular orbital (HOMO) level of the organic film is small and that the very large difference between the EA of the former and the IE of the latter is taken up by an interface dipole.<sup>8,9</sup> A schematic energy diagram of the resulting interface is illustrated in Fig. 4. Given that the oxide valence band is placed several electron-volts (2.5–3.0 eV) below the ITO Fermi level, hole injection via the VB is most unlikely. On the other hand, the  $\text{MoO}_3$  CB is only 0.6–0.7 eV above the HOMO of the organic film, and hole injection from ITO can therefore proceed via electron extraction through the CB of the oxide (Fig. 4).

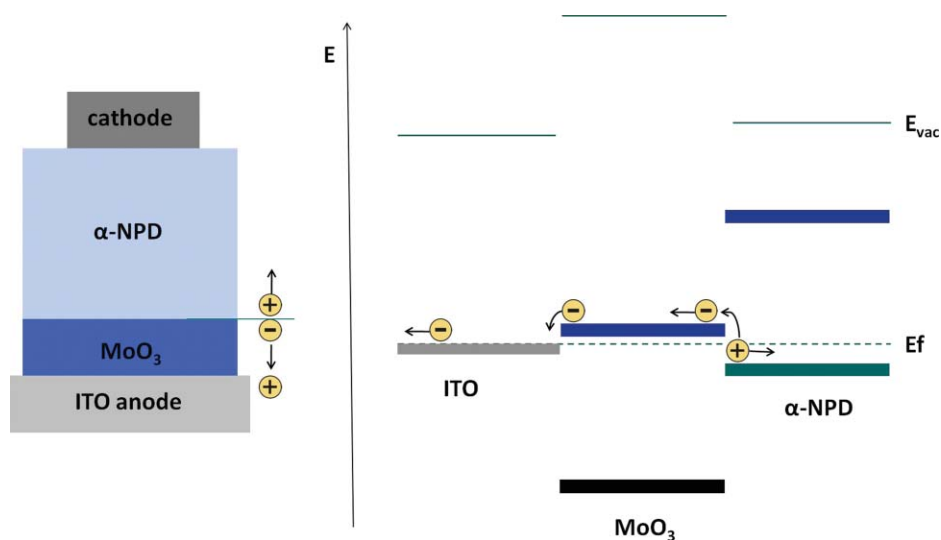


**Fig. 4** Scheme of charge injection at a  $\text{MoO}_3/\alpha$ -NPD interface.

$J$ - $V$  measurements of hole-only current injected into a polymer, TFB, from ITO with and without a hole-injection layer (HIL), are shown in Fig. 3(b).<sup>13</sup> The HIL is either a film of polyethylene dioxythiophene:polystyrene sulfonate (PEDOT:PSS, Baytron P VP CH 8000), or a MoO<sub>3</sub> film. As can be seen, MoO<sub>3</sub>, like PEDOT:PSS, considerably enhances injection. MoO<sub>3</sub>, as both exhibit sufficiently large work functions to form low hole injection barriers with the organic material. Note that the TMO, with a work function of  $\sim 5.7$  eV, in this case (exposed surface), is able to form such low barriers with organics having considerably deeper HOMO, and that greatly surpasses PEDOT:PSS. Furthermore, it surpasses the well-known doped polymer in the upper part of the  $J$ - $V$  characteristics, an indication of a significantly lower film resistivity.

As a last note, this model is not limited to charge injection and can be used to explain the charge-generation mechanism of metal-oxide-based charge generation layers (CGL). CGLs are interconnecting units used, for instance, to stack multiple OLEDs for tuning the emission color and improve device performance. It was previously proposed that such a CGL is located at the interface between the organic electron transport layer and the metal oxide. However, as illustrated in Fig. 4, the charge-generation process takes place at the metal-oxide/hole-transport interfaces, and proceeds by electron charge transfer from the HOMO of the HTL to the CB of the metal oxide. This result also confirmed that for other metal oxides, such as WO<sub>3</sub>.<sup>14,15</sup>

## 4 Conclusion

We have reviewed recent work done on the determination of the electronic structure of films of transition metal-oxide films and on the role of these materials in charge carrier injection in organic films. Clean MoO<sub>3</sub> exhibits very deep-lying energy levels with exceptionally large work function, electron affinity, and ionization energy. Contamination by air exposure leads to a  $\sim 1$ -eV reduction of these parameters; however, the hole-injection properties of the TMO films remain very efficient. The hole-injection mechanism at TMO/organic interfaces is explained by electron extraction from the HOMO level of the organic material through the oxide conduction band, also known as the charge-generation process.

## Acknowledgments

This work was supported by the Office of Science DOE Energy Frontier Research Center for Interface Science: Solar Electric Materials (Grant No. DE-S0001084), the National Science Foundation (Grant No. DMR-1005892), and the Princeton MRSEC of the NSF (Grant No. DMR-0819860). J.M. acknowledges the Deutsche Forschungsgemeinschaft for generous support within the postdoctoral fellowship program.

## References

1. K. J. Reynolds, J. A. Barker, N. C. Greenham, R. H. Friend, and G. L. Frey, "Inorganic solution-processed hole-injection and electron-blocking layers in polymer light emitting diodes," *J. Appl. Phys.* **92**, 7556–7563 (2002).
2. H. Kanno, R. J. Holmes, Y. Sun, S. Kena-Cohen, and S. R. Forrest, "White stacked electrophosphorecent organic light-emitting devices employing MoO<sub>3</sub> as charge-generation layer," *Adv. Mater.* **18**, 339–342 (2006).
3. J. Meyer, S. Hamwi, T. Bülow, H.-H. Johannes, T. Riedl, and W. Kowalsky, "Highly efficient simplified organic light emitting diode," *Appl. Phys. Lett.* **91**, 113506 (2007).
4. M. G. Helander, Z. B. Wang, M. T. Greiner, J. Qiu, and Z. H. Lu, "Substrate dependent charge injection at the V<sub>2</sub>O<sub>5</sub>/organic interface," *Appl. Phys. Lett.* **95**, 083301 (2009)
5. C.-W. Chu, S.-H. Li, C.-W. Chen, V. Shrotriya, and Y. Yang, "High-performance organic thin-film transistors with metal oxide/metal bilayer electrode," *Appl. Phys. Lett.* **87**, 193508 (2005).

6. H. You, Y. F. Dai, Z. Zhang, and D. Ma, "Improved performance of organic light-emitting diodes with metal oxide as anode buffer," *J. Appl. Phys.* **101**, 026105 (2007).
7. X. Qi, N. Li, and S. R. Forrest, "Analysis of metal-oxide-based charge generation layers used in stacked organic light-emitting diodes," *J. Appl. Phys.* **107**, 014514 (2010).
8. M. Kröger, S. Hamwi, J. Meyer, T. Riedl, W. Kowalsky, and A. Kahn, "Role of deep-lying electronic states of MoO<sub>3</sub> in the enhancement of hole-injection in organic thin films," *Appl. Phys. Lett.* **95**, 123301 (2009).
9. J. Meyer, A. Shu, M. Kröger, and A. Kahn, "Effect of contamination on the electronic structure and hole-injection properties of MoO<sub>3</sub>/organic semiconductors interfaces," *Appl. Phys. Lett.* **96**, 133308 (2009).
10. K. Kanai, K. Koizumi, S. Ouchi, Y. Tsukamoto, K. Sakanoue, Y. Ouchi, and K. Seki, "Electronic structure of anode interface with molybdenum oxide buffer layer," *Org. Elect.* **11**, 188–194 (2010).
11. D. Y. Kim, J. Subbiah, G. Sarasqueta, F. So, H. Ding, Irfan, and Y. Gao, "The effect of molybdenum oxide interlayer on organic photovoltaic cells," *Appl. Phys. Lett.* **95**, 093304 (2009).
12. C. I. Wu, Y. Hirose, H. Siringhaus, and A. Kahn, "Electron-hole interaction energy in the organic molecular semiconductor PTCDA," *Chem. Phys. Lett.* **272**, 43–47 (1997).
13. J. Meyer, R. Khalandovsky, P. Görrn, and A. Kahn, "MoO<sub>3</sub> films spin-coated from nanoparticle suspension for efficient hole-injection in organic electronics," *Adv. Mater.* **23**, 70–73 (2011).
14. J. Meyer, M. Kröger, S. Hamwi, F. Gnam, T. Riedl, W. Kowalsky, and A. Kahn, "Charge generation layers comprising metal-oxide/organic interfaces: Electronic structure and charge generation mechanism," *Appl. Phys. Lett.* **96**, 193302 (2010).
15. S. Hamwi, J. Meyer, M. Kröger, T. Winkler, M. Witte, T. Riedl, A. Kahn, and W. Kowalsky, "The role of transition metal oxides in charge generation layers for stacked organic light emitting diodes," *Adv. Funct. Mater.* **20**, 1762–1766 (2010).

Biographies and photographs of the authors not available.